UNSTEADY TWO-LAYERED CONDUCTING FLUID FLOWS THROUGH A POROUS MEDIUM BETWEEN PARALLEL PLATES IN A ROTATING SYSTEM

Supported by tetfund TERTIARY EDUCATION TRUST FUND

M. S. Dada*, A. S. Adeyemo and L. Yakub
Department of Mathematics, University of Ilorin, Kwara State, Nigeria
*Corresponding author: dadamsa@gmail.com

Received: November 02, 2017 **Accepted:** March 08, 2018

Abstract: This paper analyzes the heat transfer of a two layered rotatory fluid flow in a horizontal channel under the action of an applied magnetic and electric fields. The fluid in region one is porous of Darcy-Forchheimer type while the fluid in region two is non porous. The fluid flow is unsteady and a magnetic field is applied perpendicular to the plates. The flow is driven by a common constant pressure gradient in the channel bounded by two parallel porous insulating plates. The governing equations have been reduced to non-linear coupled ordinary differential equations by means of perturbation technique using two term series, after which Adomian Decomposition Method (ADM) was employed to solve the equations. The results are presented in graphical and tabular forms to illustrate the effects of the heat transfer characteristics and their dependence on the governing parameters. It is observed that as the Coriolis forces become stronger, the temperature decreases in both fluid regions. Furthermore, it is noticed that the temperature in the two regions diminishes with an increase in the porosity parameter. It is also seen that an increase in the Hartmann number causes decrease in the primary and secondary velocities profile.

Keywords: Adomian Decomposition Method, Coriolis force, MHD, Two-phase flow

Introduction

The magnetohydrodynamic MHD fluid system through parallel plates in a rotating medium has received the attention of many researchers due to its importance in the design of MHD generators and accelerators, geo-physics, the underground water energy storage systems, nuclear reactors, soil sciences, astrophysics. In recent years, many researchers have paid their attentions on the flow in a rotating system due to its diverse applications in many branches of science and technology. Most of the problems relating to astrophysics, geophysical fluid dynamics and aeronautics, petroleum industry and industrial applications etc, involve multi-layered fluid flow situations. Often, in the petroleum industry as well as in engineering and technological fields, a stratified two-phase or two layered fluid flow occurs. Transportation and extraction of the products of oil are other obvious applications. The results of multi-layered fluid flow studies are useful in understanding the effect of the presence of a slag layer on heat transfer characteristics of a coal fired rotating MHD generator, flow meters, in nuclear reactor and in space craft technology, etc Also, rotating flows are encountered in many industrial applications, such as in liquid metals, metal working process, geothermal energy extracts and many other applications.

The study of MHD flows through porous media has been motivated by its immense importance and hence soliciting continuous interest from researchers. Many authors have focused on the theoretical/experimental investigations of hydromagnetic flows in a rotating environment, because of their occurrence in several natural phenomena that are directly governed by the actions of the Coriolis forces and their application in various technological situations. (Ingham and Pop (2005), Nield and Bejan (2006)) have studied transport phenomena in porous media. It is worth noting that the Coriolis forces are comparable in magnitude and these Coriolis forces induce a secondary flow in the fluid, (Holton (1965), Batchelor (1967) and Gupta (1972)). Chauhan and Kumar (2009) studied the effects of slip conditions on fully developed forced convection in a circular channel filled with a highly porous medium saturated with a rarefied gas and uniform wall surface heat flux, using Darcy extended Brinkman-Forchheimer model. Considerable attention has been given to the study of an unsteady magnetohydrodynamic flow, heat transfer and their response due to the imposed oscillations/impulsive motion of a boundary or boundary temperature under the presence of an external magnetic field.

Despite these studies, the effects of unsteady two phase fluid flows through horizontal channels received much less attention in the literature. The unsteady hydromagnetic flow of electrically conducting two phase fluid flow in a rotating region over the porous boundaries gained significant theoretical and practical importance due to their applications in the petroleum industry, geophysical fluid dynamics, plasma physics, magnetohydrodynamics and in many such areas involving multi-layered fluid flows. These flows seem to be important and play interesting roles in the flow pattern as most of the practical problems dealing with immiscible fluids are unsteady in nature.

Also, in many practical problems, it is preferable to consider both immiscible fluids as electrically conducting, where one of which is highly electrically conducting compared to the other. The fluid of low electrical conductivity compared to the other is functional to reduce the power required to pump the fluid in MHD pumps and flow meters. For quite some years, emphasis has been made in research studies of two-layered fluid flows by several authors, notable amongst them are Walin (1969), Packham and Shail (1971), Debnath and Basu (1975), Michiyoshi et al. (1977) that studied unsteady two layered fluid flows. Umavathi et al (2010) examined Magnetohydrodynamics poiseuille-coutte flow and heat transfer in an inclined channel in which one region was of a conducting fluid and region two non-conducting fluid. Abdul Mateen (2013) has studied the magnetohydrodynamic flow and transient magnetohydrodynamic flow of two immiscible fluids through a horizontal channel. Ramachandra and Balaji (2014) had investigated MHD two-fluid flow and heat transfer between two inclined parallel plates in a rotating system and reported that the temperature distribution decreased as the rotation parameter increased. The unsteady radiative and MHD free convective two immiscible fluid flows through in a horizontal channel was investigated by Dada et al (2014) using the regular perturbation method and concluded that as the thermal radiation from the wall temperature decreased, the temperature profiles and thermal boundary layers increased.

Furthermore, Adeniyan and Abioye (2016) presented mixed convection radiating steady flow and heat transfer in a vertical channel partially filled with Darcy-Forcheimmer porous substrate using Adomian Decomposition method. The effects

of coriolis force was rendered insignificant. Consequently, Raju and Rao (2016) studied an unsteady two-layered fluid flow of conducting fluids in parallel porous plates under transverse magnetic field in a rotating system. However, effects of the non-linear Darcy-Forcheimmer porosity was not considered in the study for simplicity. In the present paper, magnetohydrodynamic (MHD) heat transfer in a two-layered flow of conducting Darcy-Forcheimmer porous fluids through a parallel porous plates in a rotating system in presence of an applied magnetic and electric fields is investigated theoretically. The flow is driven by a constant common pressure gradient in the channel bounded by two parallel porous plates.

Mathematical formulation of problem

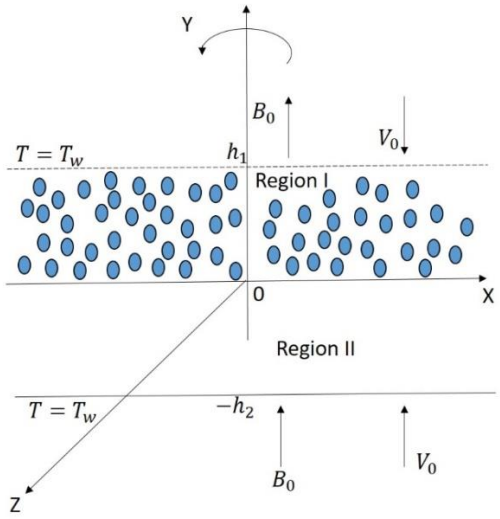

Fig. 1: Schematic diagram of the problem

The study considered two layered unsteady MHD fluid flow in a horizontal channel comprising of two infinite parallel porous plates with suction (V_o) constant and normal to these directions $y = h_1$and $y = -h_2$. The system is rotated with an angular velocity Ω in anti-clockwise direction about the y-axis perpendicular to the plates. The fluids in Region I and Region II respectively are in the upper $(0 \le y \le h_1)$ and lower $(-h_2 \le y \le 0)$regions. The x-axis is taken in the direction of hydrodynamic pressure gradient in the plane parallel to the channel plates and y-axis at right angles to the direction of flow. Figure 1 depicts the schematic flow of the problem with the origin midway between the two plates. The two bounding plates maintained constant temperature $T_{w1=}T_{w2}$. A magnetic field of uniform strength B_o is assumed to be applied transversely to the direction of flow and constant electric field E_o is applied in the z-direction. The induced magnetic field is assumed to be small when compared to an applied field, hence it is neglected. The regions are occupied by two immiscible electrically conducting, incompressible fluids with different densitiesρ_1, ρ_2, viscositiesμ_1, μ_2, electrical conductivitiesσ_1, σ_2, and thermal conductivities K_1, K_2.

The dimensional governing equations of motion and corresponding boundary conditions [Raju and Rao (2016)] for both region I and region II with an inclusion of Darcy-Forchheimer term in region one are expressed as;

Region I

$$\rho_1 \frac{\partial u_1^*}{\partial t^*} - \mu_1 \frac{\partial^2 u_1^*}{\partial y^{*2}} + \rho_{1V_0} \frac{\partial u_1^*}{\partial y^*} + \frac{\partial p}{\partial x} + \sigma_1 u_1^* B_0^2 + \sigma_1 E_0 B_0 - \frac{\mu u_1^*}{k} - \frac{b_f \rho_{1u_1^{*2}}}{k} = -2\rho_1 \Omega w_1^* \quad (1)$$

$$\rho_1 \frac{\partial w_1^*}{\partial t^*} - \mu_1 \frac{\partial^2 w_1^*}{\partial y^{*2}} + \rho_{1V_0} \frac{\partial w_1^*}{\partial y^*} + \sigma_1 w_1^* B_0^2 - \frac{\mu w_1^*}{k} - \frac{b_f \rho_{1w_1^{*2}}}{k} = 2\rho_1 \Omega u_1^* \quad (2)$$

$$\rho_1 C_{p1} \left[\frac{\partial T_1}{\partial t^*} + V_0 \frac{\partial T_1}{\partial y^*}\right] - K_1 \frac{\partial^2 T_1}{\partial y^{*2}} - \mu_1 \left[\left(\frac{\partial u_1^*}{\partial y^*}\right)^2 + \left(\frac{\partial w_1^*}{\partial y^*}\right)^2\right] - \sigma_1 u_1^{*2} B_0^2 - \sigma_1 E_0^2 = 2\sigma_1 u_1^* E_0 B_0 \quad (3)$$

Region II

$$\boldsymbol{\rho_2 \frac{\partial u_2^*}{\partial t^*} - \mu_2 \frac{\partial^2 u_2^*}{\partial y^{*2}} + \rho_{2V_0} \frac{\partial u_2^*}{\partial y^*} + \frac{\partial p}{\partial x} + \sigma_2 u_2^* B_0^2 + \sigma_2 E_0 B_0 = -2\rho_1 \Omega w_1^*} \quad (4)$$

$$\boldsymbol{\rho_2 \frac{\partial w_2^*}{\partial t^*} - \mu_2 \frac{\partial^2 w_2^*}{\partial y^{*2}} + \rho_{2V_0} \frac{\partial w_2^*}{\partial y^*} + \sigma_2 w_2^* B_0^2 = 2\rho_2 \Omega u_2^*} \quad (5)$$

$$\rho_2 C_{p2} \left[\frac{\partial T_2}{\partial t^*} + V_0 \frac{\partial T_2}{\partial y^*}\right] - K_2 \frac{\partial^2 T_2}{\partial y^{*2}} - \mu_2 \left[\left(\frac{\partial u_2^*}{\partial y^*}\right)^2 + \left(\frac{\partial w_2^*}{\partial y^*}\right)^2\right] - \sigma_2 u_2^{*2} B_0^2 - \sigma_2 E_0^2 = 2\sigma_2 u_2^* E_0 B_0 \quad (6)$$

where the subscripts 1 and 2 represent quantities for region I and region II respectively, u_1, u_2, and $w_1, w_2$are fluid velocities in x-, z-directions respectively known as primary and secondary velocity distributions. Ω is the angular velocity, T_1 and T_2 are fluid temperatures and t is the time. The boundary conditions on velocity are considered as the no-slip conditions at the lower and upper plates. The relevant interface conditions are;

$$u_1^*(h_1) = w_1^*(h_1) = 0, \text{for} t \ge 0 \quad (7)$$

$$u_2^*(-h_2) = w_2^*(-h_2) = 0 \quad (8)$$

$$u_1^*(0) = u_2^*(0),\ w_1^*(0) = w_2^*(0) \quad (9)$$

$$\mu_1 \frac{\partial u_1^*}{\partial y^*} = \mu_2 \frac{\partial u_2^*}{\partial y^*} and \mu_1 \frac{\partial w_1^*}{\partial y^*} = \mu_2 \frac{\partial w_2^*}{\partial y^*} aty = 0 \quad (10)$$

The thermal boundary and interface conditions on temperature for both fluids are given by;

$$T_1(h_1) = T_w \quad (11)$$

$$T_2(-h_2) = T_w \quad (12)$$

$$T_1(0) = T_2(0) \quad (13)$$

$$K_1 \frac{\partial T_1}{\partial y^*} = K_2 \frac{\partial T_2}{\partial y^*} aty = 0 \quad (14)$$

The following non-dimensional quantities are introduced in order to write the governing equations and the boundary conditions in dimensionless form,

$$Pr = \frac{\mu C_p}{K},\ u_1 = \frac{u_1^*}{u_p},\ u_2 = \frac{u_2^*}{u_p},\ w_1 = \frac{w_1^*}{u_p},\ w_2 = \frac{w_2^*}{u_p},\ y = \frac{y^*}{h_1}, t = \frac{Ut^*}{h_1^2}, \omega = \frac{h_1^2 \omega^* \rho}{\mu_1},\ u_p = \left(-\frac{\partial P}{\partial x}\right)\frac{h_1^2}{\mu_1},\ Da = \frac{k}{h^2},\ M^2 = \frac{B_0^2 h_1^2 \sigma_1}{\mu_1}, R_p = \frac{h_1^2 \Omega}{U_1},\ \mathcal{K} = \frac{h_1 \rho_1 V_0}{\mu_1},\ \alpha = \frac{\mu_1}{\mu_2}, h = \frac{h_2}{h_1},\ \sigma = \frac{\sigma_2}{\sigma_1},\ \beta = \frac{K_1}{K_2},\ \rho = \frac{\rho_2}{\rho_1}, R_e = \frac{E_0}{B_0 u_p}, \theta_1 = \frac{T_1 - T_w}{\frac{u_p^2 \mu_1}{K_1}},\ F_s = \frac{u_{pb_f}}{U} \quad (15)$$

where Pr is the Prandtl number, u_p is the characteristic velocity,R_e is the electric load parameter, R_p is the rotation parameter, M^2 is the magnetic parameter, Da is the Darcy number, F_s is the Forchheimer number, $\mathcal{K}$ is the porous parameter,k is *the* permeability parameter, ω is the frequency of oscillation, $\theta_1, \theta_2$are non-dimensional forms of temperature distributions of the two fluids, Ω is the angular velocity and β, σ, ρ , α, and h are the ratios of thermal conductivities, electrical conductivities, densities, viscosities and heights, respectively.

With the use of the non-dimensional quantities (15), equations (1)-(6), reduce to

REGION I

$$\frac{\partial u_1}{\partial t}-\frac{\partial^2 u_1}{\partial y^2}+\lambda\frac{\partial u_1}{\partial y}+u_1p_2+p_1-u_1^2p_{3=-2w_1R_p} \quad (16)$$

$$\frac{\partial w_1}{\partial t}-\frac{\partial^2 w_1}{\partial y^2}+\lambda\frac{\partial w_1}{\partial y}+w_1p_2-w_1^2p_{3=2u_1R_p} \quad (17)$$

$$\frac{\partial \theta_1}{\partial t}+\lambda\frac{\partial \theta_1}{\partial y}-p_0\frac{\partial^2\theta_1}{\partial y^2}-p_0\left[\left(\frac{\partial u_1}{\partial y}\right)^2+\left(\frac{\partial w_1}{\partial y}\right)^2\right]-2p_5u_1-p_5R_e-p_4u_1^2=0 \quad (18)$$

REGION II

$$\frac{\partial u_2}{\partial t}-\frac{\partial^2 u_2}{\partial y^2}+\lambda\frac{\partial u_2}{\partial y}+p_6(u_2+R_e)-p_7=-2p_8w_2R_p \quad (19)$$

$$\frac{\partial w_2}{\partial t}-\frac{\partial^2 w_2}{\partial y^2}+\lambda\frac{\partial w_2}{\partial y}+w_2p_6=2p_8u_1R_p \quad (20)$$

$$\frac{\partial \theta_2}{\partial t}+\lambda\frac{\partial \theta_2}{\partial y}-p_0\frac{\partial^2\theta_2}{\partial y^2}-p_0\frac{\beta}{\alpha}\left[\left(\frac{\partial u_2}{\partial y}\right)^2+\left(\frac{\partial w_2}{\partial y}\right)^2\right]-p_9({R_e}^2+2u_2R_e+u_2^2)=0 \quad (21)$$

where $p_1=M^2R_e-1,\ p_2=M^2-\frac{1}{Da},\ p_3=\frac{1}{Da}F_s-1,\ p_4=p_0M^2,\ p_5=p_4R_e,\ p_6=M^2\sigma h^2\alpha$

$p_7=\alpha h^2, p_8=\rho\alpha h^2, p_0=\frac{1}{Pr}, p_9=p_4\sigma h^2\beta$

The velocity, temperature and interface conditions in non-dimensional forms become:

$u_1(1)$ and $w_1(1)=0$, for $t\geq 0$ (22)

$u_2(-1)=0, w_2(-1)=0$ (23)

$u_1(0)=u_2(0), w_1(0)=w_2(0)$ (24)

$\frac{\partial u_1}{\partial y}=\left(\frac{1}{\alpha h}\right)\frac{\partial u_2}{\partial y}aty=0$ (25)

$\frac{\partial w_1}{\partial y}=\left(\frac{1}{\alpha h}\right)\frac{\partial w_2}{\partial y}aty=0$ (26)

$\theta_1(1)=0,\ \theta_2(-1)=0$ (27)

$\theta_1(0)=\theta_2(0)$ (28)

$\frac{\partial \theta_1}{\partial y}=\left(\frac{1}{\beta h}\right)\frac{\partial \theta_2}{\partial y}aty=0$ (29)

Solutions of Problem

The dimensionless governing equations (16)-(21) in both region I and II are to be solved subject to the boundary and interface conditions (22) - (29) for the primary and secondary velocities, and temperature distributions.$\lambda=\varepsilon$ is considered to be a very small term ($\varepsilon<<1$) and it is used as a perturbation parameter . The solutions are assumed in the form:

$u_1(y,t)=u_{01}(y)+\varepsilon e^{i\omega t}u_{11}(y)$ (30)

$w_1(y,t)=w_{01}(y)+\varepsilon e^{i\omega t}w_{11}(y)$ (31)

$u_2(y,t)=u_{02}(y)+\varepsilon e^{i\omega t}u_{12}(y)$ (32)

$w_2(y,t)=w_{02}(y)+\varepsilon e^{i\omega t}w_{12}(y)$ (33)

$\theta_1(y,t)=\theta_{01}(y)+\varepsilon e^{i\omega t}\theta_{11}(y)$ (34)

$\theta_2(y,t)=\theta_{02}(y)+\varepsilon e^{i\omega t}\theta_{12}(y)$ (35)

Using equations (30)-(35), the dimensionless governing equations (16) – (21) reduce to the following system of equations.

Region I

For the steady part;

$$u_{01}''=\lambda u_{01}'+p_2u_{01}-p_3u_{01}^2+p_1+2R_pw_{01} \quad (36)$$

$$w_{01}''=\lambda w_{01}'+p_2w_{01}-p_3w_{01}^2-2R_pu_{01} \quad (37)$$

$$\theta_{01}''=\frac{\lambda}{p_0}\theta_{01}'-[(u_{01}')^2+(w_{01}')^2]-\frac{u_{01}}{p_0}(2p_5+p_4u_{01})-\frac{p_5R_e}{p_0} \quad (38)$$

For the transient time dependent part;

$$u_{11}''=\lambda u_{11}'+[p_2+i\omega]u_{11}-2p_3u_{11}u_{01}+2R_pw_{11} \quad (39)$$

$$w_{11}''=\lambda w_{11}'+[p_2+i\omega]w_{11}-2p_3w_{11}w_{01}-2R_pu_{11} \quad (40)$$

$$\theta_{11}''=\frac{\lambda}{p_0}\theta_{11}'+\frac{i\omega}{p_0}\theta_{11}-2[(u_{01}'u_{11}')+(w_{01}'w_{11}')]-2p_5\frac{u_{11}}{p_0}-2\frac{p_4}{p_0}u_{11}u_{01} \quad (41)$$

Region II

For steady part;

$$u_{02}''=\lambda u_{02}'+p_6[u_{02}+R_e]-p_7+2p_8R_pw_{02} \quad (42)$$

$$w_{02}''=\lambda w_{01}'+p_6w_{02}-2p_8R_pu_{02} \quad (43)$$

$$\theta_{02}''=\frac{\lambda}{p_0}\theta_{02}'-\frac{\beta}{\alpha}[(u_{02}')^2+(w_{02}')^2]-p_9(u_{02}^2+2R_eu_{02}+R_e^2) \quad (44)$$

For the transient time dependent part;

$$u_{12}''=\lambda u_{12}'+[p_6+i\omega]u_{12}+2p_8R_pw_{12} \quad (45)$$

$$w_{12}''=\lambda w_{12}'+[p_6+i\omega]w_{12}-2p_8R_pu_{12} \quad (46)$$

$$\theta_{12}''=\frac{\lambda}{p_0}\theta_{12}'+\frac{i\omega}{p_0}\theta_{12}-2\frac{\beta}{\alpha}\left[(u_{02}'u_{12}')+w_{02}'w_{12}'\right]-2p_9(u_{02}u_{02}+R_eu_{12}) \quad (47)$$

The corresponding boundary and interface conditions on velocity and temperature become:

Steady state;

$u_{01}(1)$ *and* $w_{01}(1)=0, u_{02}(-1)$ *and* $w_{02}(-1)=0$ (48)

$u_{01}(0)=u_{02}(0),\quad w_{01}(0)=w_{02}(0)$ (49)

$\frac{du_{01}}{dy}=\left(\frac{1}{\alpha h}\right)\frac{du_{02}}{dy}$ *and* $\frac{dw_{01}}{dy}=\left(\frac{1}{\alpha h}\right)\frac{dw_{02}}{dy}$ *at* $y=0$ (50)

$\theta_{01}(1)$ *and* $\theta_{02}(-1)=0,\quad \theta_{01}(0)=\theta_{02}(0)$ (51)

$\frac{d\theta_{01}}{dy}=\left(\frac{1}{\beta h}\right)\frac{d\theta_{02}}{dy}$ *at* $y=0$ (52)

Transient time dependent;

$u_{11}(1)$ *and* $w_{11}(1)=1, u_{12}(-1)$ *and* $w_{12}(-1)=0$ (53)

$u_{11}(0)=u_{12}(0),\quad w_{11}(0)=w_{12}(0)$ (54)

$\frac{du_{11}}{dy}=\left(\frac{1}{\alpha h}\right)\frac{du_{12}}{dy}$ *and* $\frac{dw_{11}}{dy}=\left(\frac{1}{\alpha h}\right)\frac{dw_{12}}{dy}$ *at* $y=0$ (55)

$\theta_{11}(1)$ *and* $\theta_{12}(-1)=0,\quad \theta_{11}(0)=\theta_{12}(0)$ (56)

$\frac{d\theta_{01}}{dy}=\left(\frac{1}{\beta h}\right)\frac{d\theta_{02}}{dy}$ *at* $y=0$ (57)

Adomian Decomposition Method (ADM)

Adopting the standard decomposition procedure, we introduce linear differential operator and its inverse

$$L_y^2=\frac{d^2}{dy^2},\qquad L_y^{-2}(*)=\int_0^y\int_0^y(*)\,dy\,dy \quad (58)$$

$$u(y)=\sum_{n=0}^{\infty}u_n(y)\ ,\qquad w(y)=\sum_{n=0}^{\infty}w_n(y) \quad (59)$$

It may be convenient to rearrange equations (36) - (47) in operational forms as follows,

$$L_y^2u_i=g_i(y)+Ru_i+Nu_i,\qquad (i=1,2) \quad (60)$$

where the left hand side of equation (60) denotes the highest order derivative, $g_i(y)$ is the source function, Ru_i is the remainder of the linear term with derivative order less than 2, while Nu_i are nonlinear terms, equation (36) can be written as

$$u''=p_1+\lambda u'+p_2u+2R_pw-p_3u^2 \quad (61)$$

neglecting the subscript (01) for simplicity,

where $(y)=p_1,\ Ru=\lambda u'+p_2u+2R_pw, Nu=-p_3u^2$.

In an operator form, equation (61) becomes

$$L_y^2u(y)=p_1+\lambda u'++p_2u+2R_pw-p_3u^2 \quad (62)$$

Applying the inverse$L_y^{-2}$to both sides of equation (62), to have

$$L_y^{-2}L_y^2u(y)=L_y^{-2}(p_1+\lambda u'++p_2u+2R_pw-p_3u^2)$$

$$u(y)=L_y^{-2}(p_1+\lambda u'++p_2u+2R_pw-p_3u^2)$$

$$u(y) = u(0) + yu'(0) + p\frac{y^2}{2} + L_y^{-2}\left(\text{ƛ}u' + +p_2u + 2\,R_pw - p_3u^2\right) \quad (63)$$

Applying the assumed boundary conditions $u(0) = \varphi$, $u'(0) = \gamma$on equation (63), we

$$u(y) = \varphi + y\gamma + p\frac{y^2}{2} + L_y^{-2}\left(\text{ƛ}u' + p_2u + 2\,R_pw - p_3u^2\right) \quad (64)$$

substituting equation (59) into equation (64) to have,

$$\sum_{n=0}^{\infty} u_n(y) = \varphi + y\gamma + p\frac{y^2}{2} + L_y^{-2}\left[\text{ƛ}\left(\sum_{n=0}^{\infty} u_n'(y)\right) + \left(p_2\sum_{n=0}^{\infty} u_n(y)\right) + \left(2\,R_p\sum_{n=0}^{\infty} w_n(y)\right) - \left(p_3\sum_{n=0}^{\infty} u_n^2(y)\right)\right]$$

i.e

$$\sum_{n=0}^{\infty} u_n(y) = \varphi + y\gamma + p\frac{y^2}{2} + L_y^{-2}\begin{bmatrix}\text{ƛ}\left(\sum_{n=0}^{\infty} u_n'(y)\right) + \left(p_2\sum_{n=0}^{\infty} u_n(y)\right) + \\ \left(2\,R_p\sum_{n=0}^{\infty} w_n(y)\right) - \left(p_3\sum_{n=0}^{\infty} A_n(y)\right)\end{bmatrix} \quad (65)$$

where A_n is the Adomian polynomial for the non-linear term $F(u)$ which is expressed as;

$$\sum_{n=0}^{\infty} A_n = u_n^2$$

It can be evaluated using the general formula

$$A_n = \frac{1}{n!}\frac{d^n}{d\Upsilon^n}\left[F\left(\sum_{i=0}^{n}\Upsilon^i u_i\right)\right]_{\Upsilon=0} \qquad n = 0,1,2,3 \ldots \quad (66)$$

For n ≥ 1, the recursive relation of equation (65) takes the form

$$u_{n+1} = \varphi + y\gamma + p\frac{y^2}{2} + L_y^{-2}\left(\text{ƛ}u_n' + +p_2u_n + 2\,R_pw_n - p_3u_n^2\right) \quad (67)$$

From equation (67), the initial approximation is

$$u_0 = \varphi + y\gamma + p\frac{y^2}{2} \quad (68)$$

When $n = 0$,

$$u_1 = L_y^{-2}\left(\text{ƛ}u_0' + p_2u_0 + 2\,R_pw_0 - p_3u_0^2\right) \quad (69)$$

Similarly, equations (37) - (47) are transformed into operator form as done with equation (36) solving for the general recurrence solution as in equation (36) and the set of equations are encompassed in a computer algebraic language using Mathemtica-16 software package for simulations system of equations and then implemented for parametric values of the emerging flow parameters. Using the assumed solution in equations (30)-(35), the results of the primary and secondary velocities with the temperature of region one and two are expressed graphically for fixed values ($\omega = 0.5, \varepsilon = 0.005, Fs = 1.5, M^2 = 0.2, \beta = 0.5, \sigma = 0.5, h = 2, R_e = -1, R_p = 1, \rho = 2,\ \omega t = 45, Pr = 4$)

The skin friction at the upper plate is given by;

$$\tau_u = \left[\left(\frac{du_{01}}{dy}\right)_{y=1} + \varepsilon e^{i\omega t}\left(\frac{du_{11}}{dy}\right)_{y=1}\right] \quad (70)$$

while at the lower plate is given by:

$$\tau_l = \left[\left(\frac{du_{02}}{dy}\right)_{y=1} + \varepsilon e^{i\omega t}\left(\frac{du_{12}}{dy}\right)_{y=1}\right] \quad (71)$$

The heat transfer rate (Nusselt number) at the upper plate is given by;

$$Nu_u = \left[\left(\frac{\theta_{01}}{dy}\right)_{y=1} + \varepsilon e^{i\omega t}\left(\frac{\theta_{11}}{dy}\right)_{y=1}\right] \quad (72)$$

The heat transfer rate (Nussel tnumber) at the lower plate is given by;

$$Nu_l = \left[\left(\frac{\theta_{02}}{dy}\right)_{y=1} + \varepsilon e^{i\omega t}\left(\frac{\theta_{12}}{dy}\right)_{y=1}\right] \quad (73)$$

Results and Discussion

Unsteady two layered conducting fluid flows through a porous medium between two parallel plates in a rotating frame has been investigated, the resulting differential equations are solved using perturbation method with Adomian Decomposition method. Solutions for the primary and secondary velocities with the temperature profile distributions in the two fluid regions, namely $u_1, u_2, w_1, w_1$and $\theta_1, \theta_2$are presented graphically for small value of ε, the coefficient of exponent of periodic frequency parameter. In the absence of Darcy number and Forchheimer number, the results are in agreement with that of Raju and Rao (2016). The corresponding profiles are plotted after obtaining the computational values for different sets of values of the governing parameters involved, such as the Hartmann number M^2, Taylor number (rotation parameter) R_p, suction number (porous parameter) ƛ, ratios of the heights h, Forchheimer number Fs. The results are depicted graphically in Figs. 2-18 for the primary and secondary distributions in Region I and Region II. Also, the effects of the coefficient of the skin friction and the Nusselt number at the upper and lower plate on each governing parameter are shown in Table 1.

Table 1: Skin friction and Nusselt number at the upper plate and lower plate with variation of each dimensionless parameter

Pr	ε	ρ	R_e	α	M	Da	β	Fs	τ_U	τ_L	Nu_U	Nu_L
4	0.005	2	3.0	1.00	0.2	1.5	0.5	1.5	2.3030	0.9854	1.8191	5.8252
4	0.007	2	3.0	1.00	0.2	1.5	0.5	1.5	2.3036	0.9845	1.8183	5.8321
4	0.009	2	3.0	1.00	0.2	1.5	0.5	1.5	2.3047	0.9827	1.8168	5.8459
6	0.005	2	3.0	1.00	0.2	1.5	0.5	1.5	2.1111	0.9886	1.0510	5.8269
8	0.005	2	3.0	1.00	0.2	1.5	0.5	1.5	2.0966	0.9883	1.1524	5.5697
4	0.005	2.5	3.0	1.00	0.2	1.5	0.5	1.5	2.2765	1.2643	3.0934	10.1240
4	0.005	3	3.0	1.00	0.2	1.5	0.5	1.5	2.2547	2.1575	4.4891	14.5850
4	0.005	2	3.5	1.00	0.2	1.5	0.5	1.5	2.2904	0.9738	1.8482	5.7689
4	0.005	2	4.5	1.00	0.2	1.5	0.5	1.5	2.2711	0.9418	1.9454	5.7548
4	0.005	2	3.0	1.05	0.2	1.5	0.5	1.5	2.3009	1.0022	1.8690	5.9587
4	0.005	2	3.0	1.09	0.2	1.5	0.5	1.5	2.3076	1.1267	2.2687	7.3967
4	0.005	2	3.0	1.00	0.5	1.5	0.5	1.5	2.0140	0.5530	1.9611	3.7394
4	0.005	2	3.0	1.00	0.6	1.5	0.5	1.5	1.9450	0.4449	2.1500	3.3396
4	0.005	2	3.0	1.00	0.2	2.0	0.5	1.5	2.3028	0.9891	1.7116	5.5289
4	0.005	2	3.0	1.00	0.2	3.0	0.5	1.5	2.3112	0.9894	1.6148	5.2803
4	0.005	2	3.0	1.00	0.2	1.5	0.7	1.5	2.3000	0.9899	2.1371	8.0575
4	0.005	2	3.0	1.00	0.2	1.5	0.9	1.5	2.3000	0.9899	2.3621	10.3146
4	0.005	2	3.0	1.00	0.2	1.5	0.5	1.65	2.3040	0.9898	1.8379	5.8158
4	0.005	2	3.0	1.00	0.2	1.5	0.5	1.75	2.3112	0.9894	1.6148	5.2803

Figures 2 and 10 show the effects of Hartmann number M^2on primary and secondary velocities, respectively. Increasing Hartmann number M^2, slow down both the primary and secondary velocities. It is due to the fact that an increase in applied magnetic field strength produces greater interaction between the fluid motion and the magnetic field, thereby increasing the Lorentz force. This force opposes the buoyancy force, causing a reduction in the velocities.

Figures 3 and 7 demonstrate the effects of varying the porous parameter (suction number) ƛ on the primary and secondary velocities on the two fluid regions. It is observed that an increase in ƛ diminishes the primary and secondary velocity distributions in both fluid regions. This is due to the fact that

when the suction number increases, the velocity components reduce.

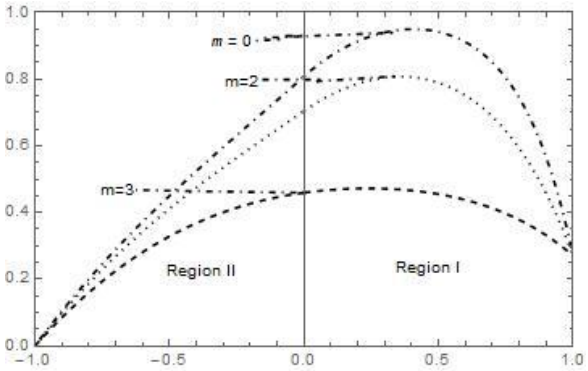

Fig. 2: Primary velocity profiles for different values of Hartmann number

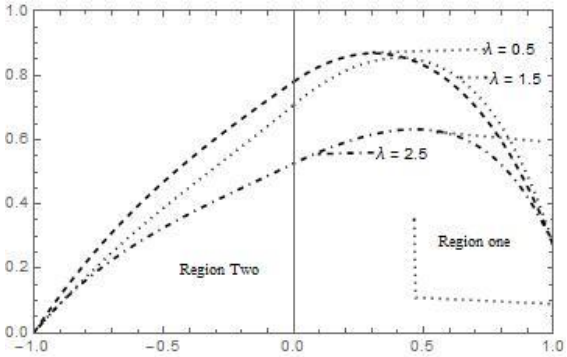

Fig. 3: Primary velocity profiles for different values of suction parameter

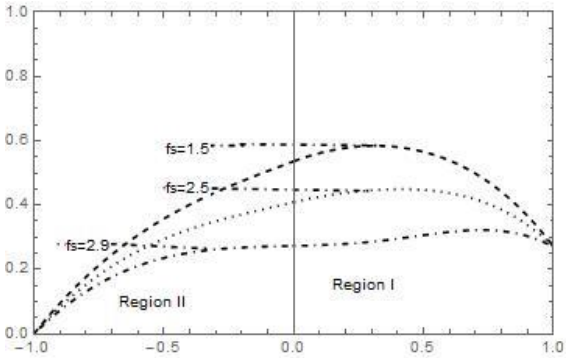

Fig. 4: Primary velocity profiles for different values of Forchheimer number Fs

Figures 4 and 9 show the effects of the Forchheimer number Fs on primary velocities and secondary velocities respectively. Also, increasing the Forchheimer number consequently features a little fall or decrease in the velocity profiles.

The effects of rotation parameter on primary velocity u and secondary velocity w respectively can be seen in Figs. 6 and 8. From the figures, it is evident that increasing rotation parameter caused low rise in velocity profile. The rotation parameter R_p defines the relative magnitude of the Coriolis force and the viscous force in the regime. As the high magnitude Coriolis forces oppose the buoyancy force, the velocity will be decreased as shown in the Fig. 6 and 8.

Figures 5 and 11 represent the effects of the ratio of heights h on primary and secondary velocities, respectively. The higher the height, the lower its velocities on both primary and secondary velocities profiles on both regions. Fig. 12 represents the effect of Hartmann number M^2 on the temperature profile. From the figure, it is clear that the effect of increasing M^2 is to decrease in the temperature profile. The effect of rotation parameter on temperature can be seen in Fig. 13. From the figure, it is evident that the temperature decreases with the increase in the rotation parameter. As the high magnitude Coriolis forces oppose the buoyancy force, the velocity will be decreased leading to a reduction in the viscous and Joule dissipation and so to a reduction in the temperature.

Figure 14 demonstrates the effect of varying the porous parameter (suction number) on the temperature distribution in the two fluid regions. It is observed that an increase in porous parameter diminishes the temperature distribution in both fluid regions. This is due to the fact that, when the suction number increases, the velocity components become thin and hence a decrease in temperature distribution. Fig. 15 exhibits the effect of varying the thermal conductivity ratio on the temperature distribution. It is observed that an increasing β speeds up the temperature distribution in the two fluid regions and Figs. 16 and 18 shows the effect of varying viscosity ratio and electrical conductivity. It is found that an increase in viscosity ratio and electrical conductivity diminishes the temperature profiles.

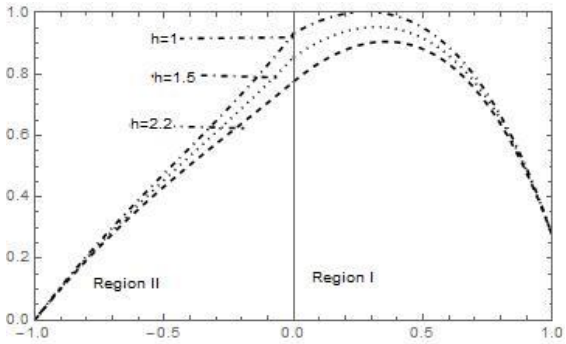

Fig. 5: Primary velocity profiles for different values of ratio of heights h

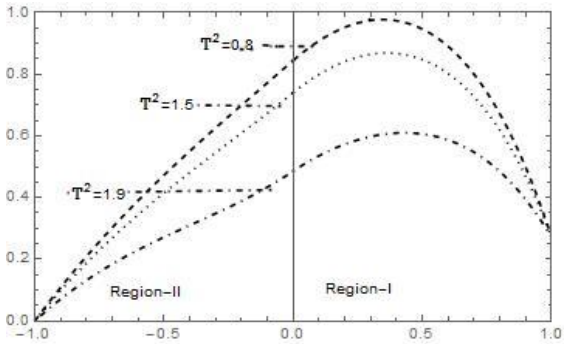

Fig. 6: Primary velocity profiles for different values of rotation parameter

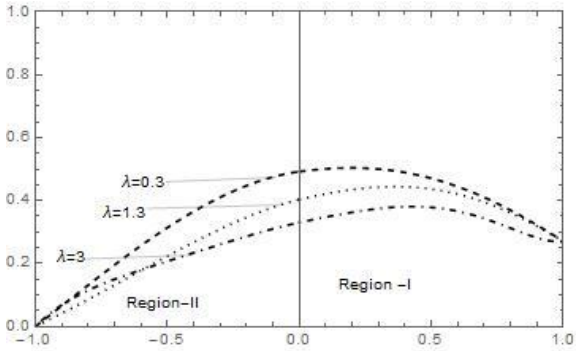

Fig. 7: Secondary velocity profiles for different values of suction parameter

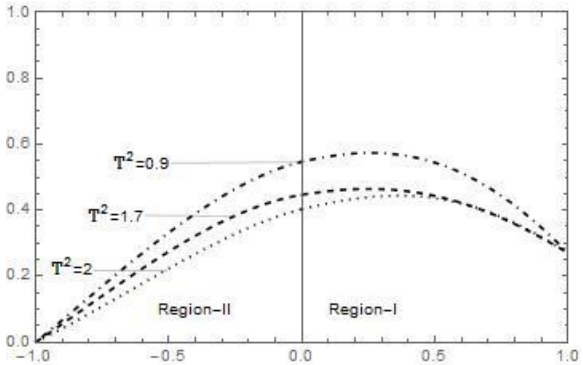

Fig. 8: Secondary velocity profiles for different values of Rotation parameter

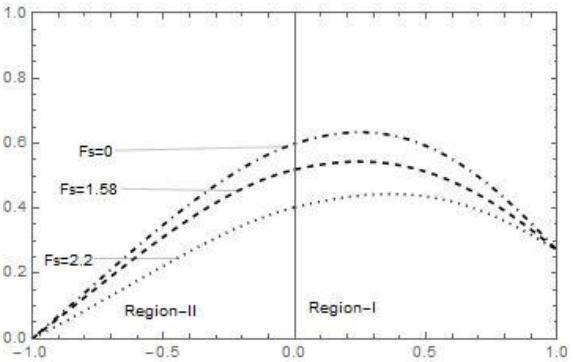

Fig. 9: Secondary velocity for different values of Forchheimer number *Fs*

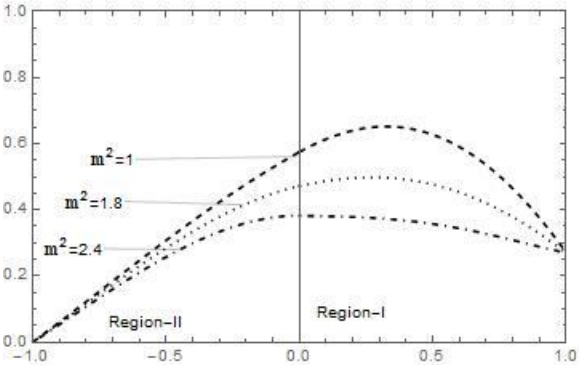

Fig. 10: Secondary velocity for different values of Hartmann number

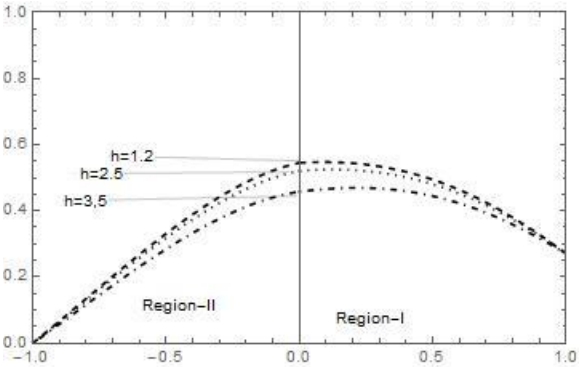

Fig. 11: Secondary velocity for different values of ratio of heights

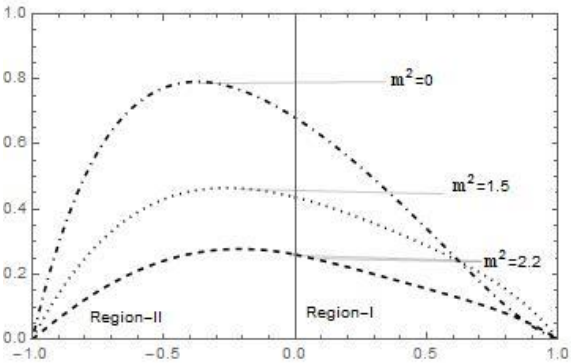

Fig. 12: Temperature profiles for different values of Hartmann number

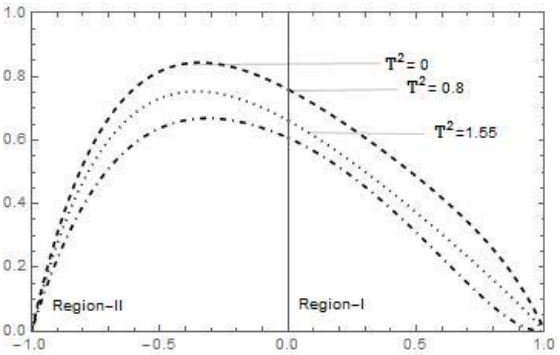

Fig. 13: Temperature profiles for different values of rotation parameter

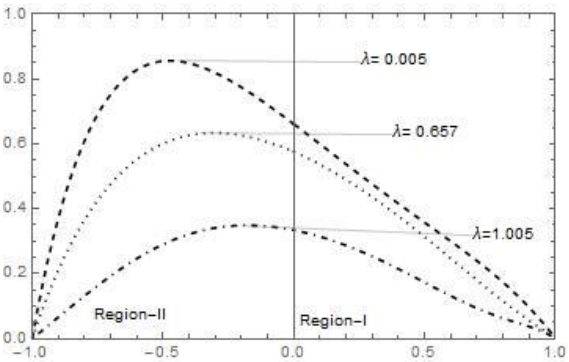

Fig. 14: Exhibits the effect of different values of porous parameter on temperature distributions on both region

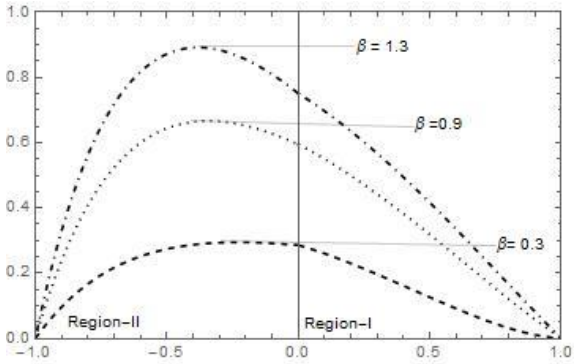

Fig. 15: Temperature profiles for different values of ratio of thermal conductivity

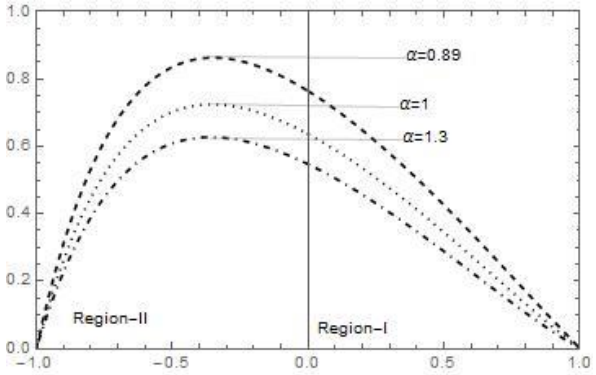

Fig. 16: Temperature profiles for different values of ratio of viscosities

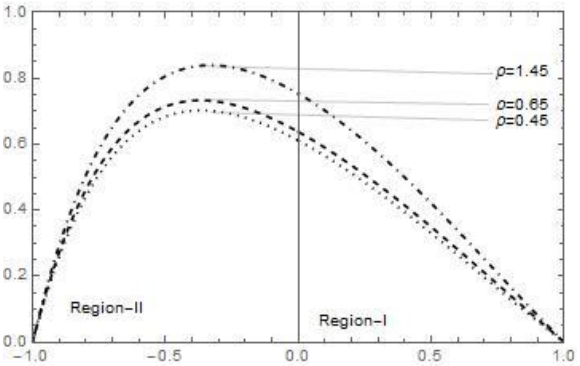

Fig. 17: Temperature profile for different values of ratio of densities

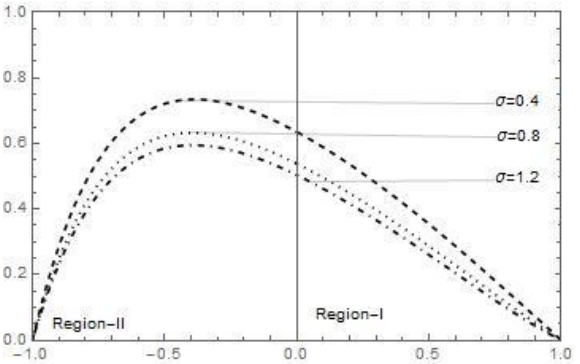

Fig. 18: Temperature profiles for different values of ratio of electrical conductivities

Table 1 shows the magnitude of the coefficient of skin friction and the nusselt number at the upper and lower plate due to the variations in the basic governing parameters. It can be seen that the coefficient of the skin friction at the upper and lower plate decreases with an increase in the Hartmann number, Prandtl number, electric load parameter and density ratio while it increases with an increase in Darcy number and ratio of viscosity. Also, the coefficient of skin friction increases at the upper plate and decreases at the lower plate due to increase in the Forchheimer number meanwhile the ratio of thermal conductivity has no effect on the coefficient of skin friction. Furthermore the Nusselt number decreases at the upper and lower plates with an increase in Prandtl, whereas Forchheimer and Darcy numbers increases when ratios of density, thermal conductivity and viscosity are increased. Moreover, the Nusselt number at the upper plate increases in value with an increase in electric load parameter and Hartmann number while it decreases at the lower plate.

Conclusion

The problem of an unsteady magnetohydrodynamic (MHD) flow of two layered porous fluids through horizontal channel bounded by two parallel porous plates in a rotating frame of reference is analyzed theoretically. The analytical solutions of the governing equations are evaluated numerically. The combined effect of the magnetic field and coriolis force in porous channels on the primary, secondary and temperature profiles in both the fluid regions are also discussed. It is found that an increase in the Hartmann number, suction parameter, rotation parameter and Forchheimer number (M^2, Λ, R_p and Fs) causes a decrease in the primary, secondary velocities and temperature profile in the two regions for fixed values of the remaining parameters involved. It is observed that as the coriolis forces become stronger, the temperature decrease in both fluid regions. It is also seen that, an increase in porous parameter diminishes the temperature distribution in both regions. It is noticed that the temperatures in the two regions increases with an increase in thermal conductivities and densities in both regions while temperature diminishes as ratio of viscosities increases.

Conflict of Interest

The authors declare that there is no any form of conflict interest regarding this publication or whatsoever.

References

Abdul Mateen 2013. Magnetohydrodynamic flow and heat transfer of two immiscible fluids through a horizontal channel. *Int. J. Current Engr. & Techn.*, 3: 1952–1956.

Adeniyan A & Abioye IA 2006. Mixed convection radiating flow and heat transfer in a vertical channel partially filled with a Darcy Forchheimer porous substrate. *Gen. Math. Notes*, 32(2): 80-104.

Batchlor GK 1967. *An Introduction to Fluid Dynamics*. I Edition, Cambridge press, Cambridge, UK.

Chauhan DS & Kumar V 2009. Effects of slip conditions on forced convection and entropy generation in a circular channel occupied by a highly porous medium: Darcy extended Brinkman-Forchheimer model. *Turkish J. Eng. Env. Sci.*, 33:91-104.

Dada MS, Onwubuoya C & Joseph KM 2014. The unsteady radiative and MHD free convective two immiscible fluid flows through in a horizontal channel. *Nig. J. Pure & Appl. Sci.*, 27: 2562-2577.

Debnath L & Basu U 1975. Unsteady slip flow in an electrically conducting two-phase fluid under transverse magnetic fields. *NUOVO Cimento*, 28: 349-362.

Gupta AS 1972. Magnetohydrodynamic Ekmann layer. *Acta Mechanica*, 13: 155-176.

Holton JR 1965. The influence of viscous boundary layers on transient motions in a stratified rotating fluid. *Int. J. Atmospheric Sci.*, 22: 402-417.

Ingham DB & Pop I 2005. *Transport Phenomena in Porous Media*, Elsevier, Oxford, UK.

Michiyoshi Funakawa Kuramoto C, Akita Y & Takahashi O 1977. Instead of the helium-lithium annular-mistflow at high temperature, an air-mercury stratified flow in a horizontal rectangular duct in a vertical magnetic field. *Int. J. Multiphase Flow*, 3: 445-463.

Nield DA & Bejan A 2006. *Convection in Porous Media (3rd Ed.)*, Springer Science Business Media, Inc., New York.

Packham BA & Shail R 1971. Stratified laminar flow of two immiscible fluids. *Proceedings of Cambridge Philosophical Society*, 69: 443-448.

Raju TL & Rao BN 2016. MHD Heat transfer in two layered flow of conducting fluids through a channel bounded by two parallel porous plates in a rotating system. *Int. J. Appl. Mechanics & Engr.*, 21(3): 623-648.

Sri RM & Balaji P 2014. MHD two-fluid flow and heat transfer between two inclined parallel plates in a rotating system. *Int. Scholarly Res. Notices*, 2: 1-11.

Umavathi JC, Liu IC & Prathap KJ 2010. Magnetohydrodynamic poiseuille-couette flow and heat transfer in an inclined channel. *Journal of Mechanics*, 26(4): 525-532.

Walin G 1969. Some aspects of time dependent motion of a stratified rotating fluid *Journal of Fluid Mechanics*, 36: 289-308.